PHYSICAL REVIEW B VOLUME 55, NUMBER 24 15 JUNE 1997-II

Photoelectron diffraction evidence for a surface substitutional site of Sb in the Sb-induced smooth growth of Ag on Ag(111)

H. Cruguel, B. Lépine, S. Ababou, F. Solal, and G. Jézéquel
UMR-CNRS-Université 6627, Physique des Atomes, Lasers, Molecules et Surfaces, Equipe surfaces-interfaces, Av. Gal. Leclerc, 35042 Rennes-Cédex, France

C. R. Natoli
Laboratori Nazionale Frascati, INFN, Via E. Fermi, 40, Cassella Postale 13-00044 Frascati, Italy

R. Belkhou
LURE, 91405 Orsay-Cédex, France

(Received 2 April 1997)

We apply low-energy photoelectron diffraction to study the crystalline site of Sb, either adsorbed onto Ag(111) or segregated on its surface after silver homoepitaxy. The experimental data are interpreted in the framework of full multiple-scattering theory with complex potentials for different Sb positions. We conclude in favor of a surface substitution site for Sb, and we also draw some conclusions about the Sb-Sb environment. Our findings seem to corroborate the suggestion put forward by Vrijmoeth *et al.* [Phys. Rev. Lett. **72**, 3843 (1994)] regarding the Sb-induced smooth growth of Ag on Ag(111). [S0163-1829(97)50124-X]

This study has been motivated by the growing interest in the mechanism of surfactant-induced layer-by-layer epitaxial growth. On the one hand, the surfactant effect of a fraction of a monolayer (0.2 ML) of Sb has been clearly demonstrated in the case of Ag on an Ag(111) surface.[1] On the other, total-energy calculations, using the linear muffin-tin orbital—local-density-approximation scheme[2] and comparing several Sb adsorbate configurations in a silver matrix, provide theoretical evidence for the occurrence of a Sb substitutional site right at the surface and the formation of a disordered Ag-Sb surface alloy. Consequently Sb should act as a repulsive site for Ag adatoms, reducing the surface mobility and leading to an increase of island density during growth. In this way the critical island cluster size beyond which three-dimensional growth occurs is not achieved.[3] It was suggested that reducing the islands' dimensions without reducing the adatom mobility on their summits would result in enhanced interlayer mass transport and layer-by-layer growth. In fact, it was proposed ''that Sb would only move up to the next growing layer upon coalescence of the former so that the mobility on top of the islands would not be reduced.''

This picture was put under scrutiny by Vrijmoeth *et al.*[4] in a scanning-tunnel-microscope study of the surfactant effect of Sb on Ag(111). These authors found evidence of embedded Sb atoms at the surface of both terraces and islands during growth, thus showing that Sb atoms segregate to the top before one layer of Ag adatoms is completed. Based on this they suggested an alternative mechanism whereby the additional edge barrier (the barrier to descend a step minus the surface diffuse barrier) is reduced by a concomitant reduction of the mobility on terraces, islands, and along step edges.

With the aim of bringing conclusive evidence to this debate, we have performed a low-energy photoelectron diffraction (LEPD) study of Sb-induced smooth growth of Ag on Ag(111). In this way, we hope to provide direct and convincing evidence that during the homoepitaxial growth Sb always occupies a substitutional surface site over the whole surface (islands and terraces) corroborating the view contained in Ref. 4. LEPD is the technique of choice for such a study, since the advantage of the selectivity for starting from the initial Sb $4d$ core level adds to the greater sensitivity of the escaping photoelectron to the short-range environment, both chemical and geometrical, due to the quasi-isotropy and atom sensitivity of the atomic scattering factor at low kinetic energy. Indeed this state of affairs parallels the situation encountered in the near-edge x-ray absorption spectroscopy[5] with the additional advantage in LEPD that one can perform not only energy scans but also polar and/or azimuthal angle scans. The price to pay for these advantages is the use of full multiple-scattering (MS) calculations in order to interpret the data as the MS perturbation expansion does not necessarily converge at low photoelectron energy. It is worthwhile noticing that, in this regime, except for symmetry considerations, there is no direct information coming from the data. Only comparison with calculations allows one to draw definite conclusions.

The sample preparation procedure is very similar to the one used by Vrijmoeth *et al.*[4] and should result in terraces of 1 μm size. We collected data from a fraction c of monolayer (from one sample to the other, the value of c is between 0.23 ± 0.02 ML and 0.26 ± 0.02 ML) of Sb deposited on a clean Ag(111) surface before and after deposition of various thicknesses of silver. It appears that a weak reconstruction is observed by low-energy electron diffraction (LEED) provided that the sample is maintained at temperature greater than 400 K during the Sb deposition, and this is true even if Sb deposition is followed by Ag deposition.

Prior to the low-energy photoelectron diffraction experiments themselves, we performed x-ray photoelectron diffraction (XPD) (high-energy regime) in the polar angle scan

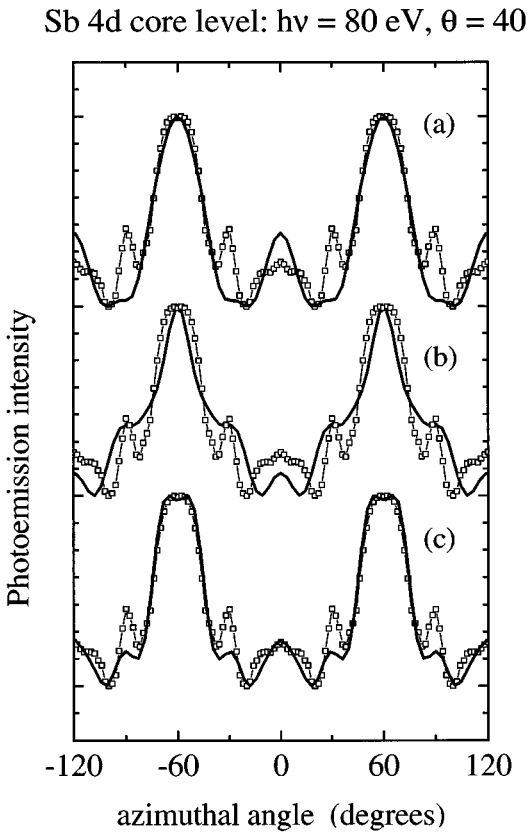

FIG. 1. Comparison between experimental data taken at $h\nu = 80$ eV and calculations for the case of (a), (b), and (c) configurations. *R*-factor values are equal to (a): 0.05, (b): 0.05, (c): 0.02.

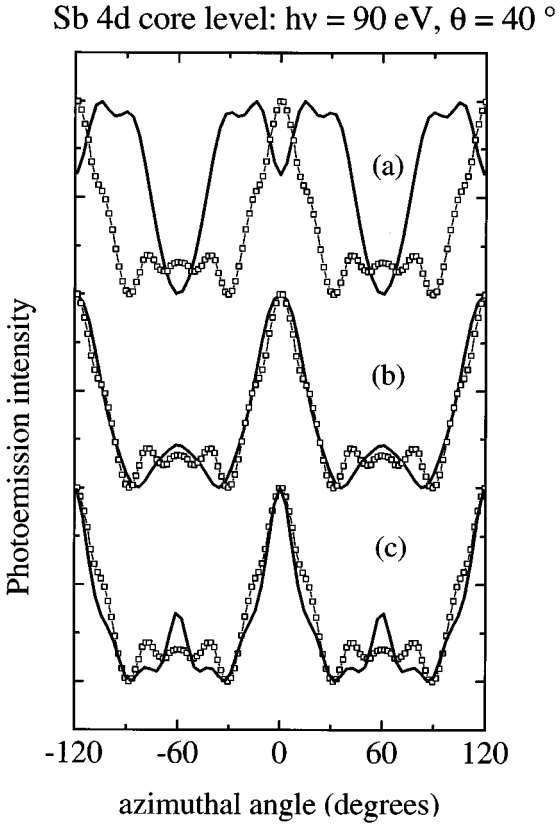

FIG. 2. Comparison between experimental data taken at $h\nu = 90$ eV and calculations for the case of (a), (b), and (c) configurations. *R*-factor values are equal to (a): 0.36, (b): 0.015, (c): 0.027.

mode, in order to investigate the possible incorporation of Sb during the silver growth procedure. The insignificant evolution of the Sb 4*d* core-level emission intensity (within 15%) with increasing thicknesses of silver together with the absence of XPD modulations, indicates an absence of evaporation or incorporation of Sb after deposition of silver up to 50 ML. This absence of incorporation is a prerequisite for any species to act as a surfactant.

The main experiment, namely the measurements of the photoelectron diffraction modulations of Sb 4*d* core-level emission, was performed at LURE, the French synchrotron radiation facility at Orsay using the 7 m toroidal grating monochromator of beam line SA73. The data, taken either from a deposit of Sb or from the same deposit of Sb followed by Ag, coverages up to 50 ML, are not significantly different. The data we discuss here were taken on samples for which Sb deposition is followed by a 10 ML deposit of Ag. From the whole set of collected data, we will only discuss the intensity modulations of Sb 4*d* core-level emissions with respect to the azimuthal angle, measured at photon energies of 90 and 80 eV. The polar angle was chosen as 40°. In all cases, the Sb 4*d* core-level photoemission spectrum shows a single multiplet component. No evidence is found therefore for different kinds of sites. The resulting modulations are shown in Figs. 1 and 2. They have been averaged and symmetrized, taking into account the $C3v$ symmetry that appeared clearly in the raw data.

In order to find out the site where Sb sits at the surface, we have performed full MS calculations[5,6] to compare with the experimental data. The calculations take into account the multiple-scattering processes to any order within a given cluster and automatically incorporate a final-state photoelectron mean-free path via a complex optical potential of the Hedin-Lundquist type. This kind of approach has been successfully applied to the determination of the relaxation of InP(110) and Si(100) clean surfaces.[6,7] In our model, the linear dimension of the hemispherical cluster around the photoemitter has been taken equal to 13 Å, which is large enough to reach size convergence, since this distance is more than twice the photoelectron mean-free path at the selected experimental conditions.

The construction of the charge density and potential necessary to the calculations follow the same patterns as in Ref. 8. Full inversion of the MS matrix was performed, since, at the kinetic energy of the photoemitted electrons (45 or 55 eV), the MS series did not converge. The calculations take complete advantage of the symmetry group of the model cluster in order to reduce the size of the MS matrix to be inverted. Based on the apparent $C3v$ symmetry of the raw data, we have only considered configurations with this point group. The absence of XPD modulations and the conservation of Sb 4*d* intensity after silver deposition are two good reasons to explore sites at the surface only or at least near to the surface. We compare therefore, three situations namely, a fcc stacking adatom site [configuration (a) in all the following figures], a substitution site in the second layer below the surface [configuration (b)], and substitution right at the sur-

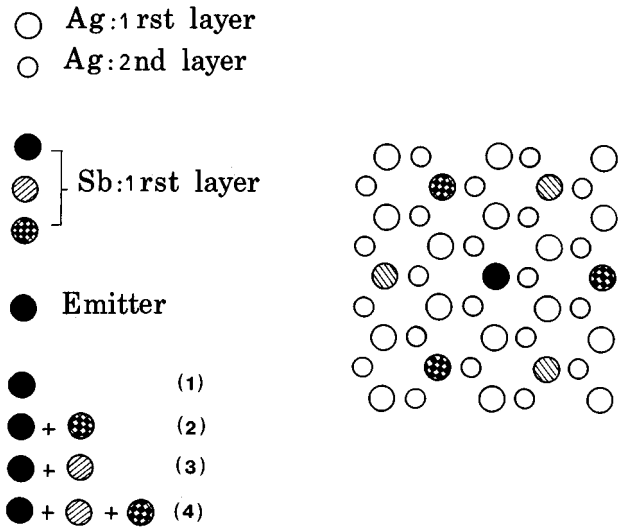

FIG. 3. Description of the (1), (2), (3), and (4) Sb second-neighbor environments. Azimuthal angle equal to zero corresponds to the horizontal direction in this figure.

face [configuration (c)]. We have also performed step sites model calculations and find poor agreement with the experimental data. It is estimated that more than 15% of Sb sitting on these sites would quantitatively deteriorate the agreement discussed below.

For the three configurations (a), (b), and (c), Figs. 1 and 2 compare the calculations with the corresponding experimental data, respectively, in the case of 80 and 90 eV photon energy. The fit parameters, although not completely uncorrelated, are the photoelectron kinetic energy inside the crystal, the inner potential and the internal polar angle. The goodness of the fit was checked by minimizing a normalized R factor[9] for each configuration. The resulting sets of parameters are very similar from one configuration to the other. In addition the 80 and 90 eV sets of parameters are fully consistent and the deduced emission angles (internal angle of 32° versus external angle of 40° in the case of the 90 eV data) agree with simple refraction rules. No antimony environment is taken into account in this preliminary modeling. The corresponding R factors are given in the figure captions. Clearly configuration (a) is ruled out, especially on the basis of the 90 eV data. Configuration (b) gives poor agreement with the 80 eV data with a bad R-factor value. In addition, in the case of the 90 eV data and despite a good R-factor value most of the experimental features are missing, namely the triplet feature around 60° azimuthal angle and the shoulder of the 0° feature. On the contrary, in the case of the surface substitution site (c) all the features appear, the corresponding R factors are very good, and this site gives the best R factor for the 80 eV data. This surface substitution site appears thus as the best candidate. In addition, taking into account the Sb environment substantiates this conclusion as discussed in the following section.

We are induced by LEED and by LEPD observations to consider the kind of $C3v$ environment depicted in Fig. 3. Only at emitter surface substitutional sites will be consid-

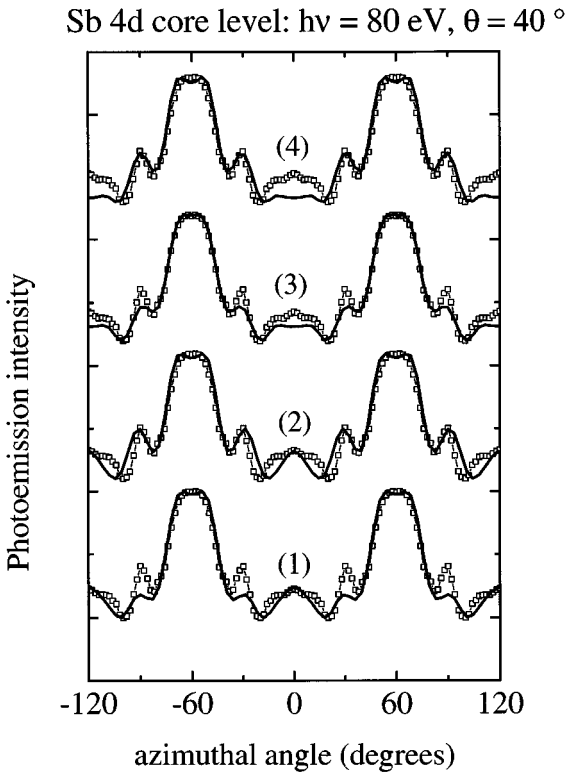

FIG. 4. Comparison between experimental data taken at $h\nu = 80$ eV and calculations for the case of environment (1), (2), (3), and (4). R-factor values are equal to (1): 0.018, (2): 0.018, (3): 0.01, (4): 0.02.

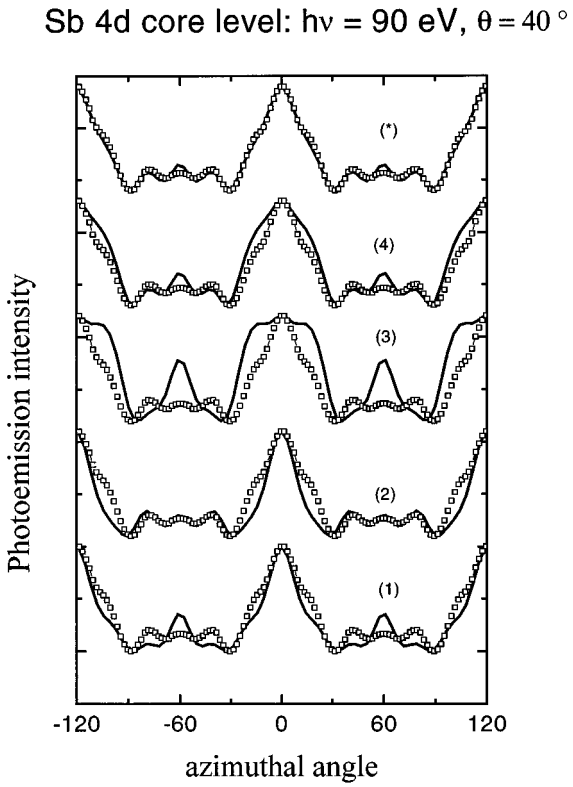

FIG. 5. Comparison between experimental data taken at $h\nu = 90$ eV and calculations in the case of environment (1), (2), (3), and (4). The (*) configuration is a mixture of configurations (2) and (4). R-factor values are equal to (1): 0.027, (2): 0.043, (3): 0.1, (4): 0.024, (*): 0.01.

ered, since other emitter configurations with the same environment give much worse R factors. Configuration (1) is the same as configuration (a) already considered. As apparent from Figs. 4 and 5, configuration (2) reproduces most of the spectral patterns with the right intensity, namely the 0° maximum and the 60° triplet, both at 80 and 90 eV photon energies. Configuration (3) competes with (2) at 80 eV but is definitely worse at 90 eV. Configurations (2) and (3) are equivalent from the point of view of the first layer only, but differ if the subsurface layer is considered. They should energetically differ through effective triplet interaction and our data indicate that configuration (2) is favored with respect to (3). At a coverage of 0.16 ($=1/6$) ML only configuration (2) would be mainly occupied. Adding more Sb atoms forces them to occupy configuration (3) so that configuration (4) builds up. This latter is in fact the configuration that reproduces, at best, the triplet feature around 60° and allows a symmetrical shoulder to grow up on the central peak at 0°. A mixture of around 40% of configuration (2) and 60% of configuration (4) should provide the best fit to the data [(∗) in Fig. 5]. This leads to a coverage of 0.27 ML very close to the experimental coverage, which is estimated for this sample to be 0.25 ± 0.02 ML. Together with the fact that the experimental data are similar, irrespective of the number of Ag layers added, this is a direct evidence that Sb is spread uniformly over both islands and terraces. Finally, we have also explored the possibility of relaxation of the Sb atomic positions. Relaxation has a very strong effect on the photocurrent modulation, since it modifies the bondings angles in a way different from all the various sites and environments considered above. No real improvement is found by relaxing the atomic Sb position either up from or down towards the surface. Although theoretical calculations suggest that an upwards relaxation of about 5% is expected, no evidence is found in this study to substantiate this.

In conclusion, using LEPD we have shown that during the homoepitaxial growth of Ag on Ag(111), Sb always occupies a substitutional surface site over the whole surface, irrespective of the number of Ag layers added, up to 50 ML, corroborating in a direct way the finding of Ref. 4. This study gives unique evidence for the formation of a Sb-Ag surface alloy and information about the resulting local chemical order.

[1] H. A. van der Vegt, H. M. van Pinxteren, M. Lohmeier, E. Vlieg, and J. M. C. Thorton, Phys. Rev. Lett. **68**, 3335 (1992).

[2] S. Oppo, V. Fiorentini, and M. Scheffer, Phys. Rev. Lett. **71**, 2437 (1993).

[3] V. Fiorentini, S. Oppo, M. Scheffer, Appl. Phys. A **60**, 399 (1995); J. Tersoff, A. W. Denier van der Gon, and R. M. Tromp, Phys. Rev. Lett. **72**, 266 (1994).

[4] J. Vrijmoeth, H. A. van der Vegt, J. A. Meyer, E. Vlieg, and R. J. Behm, Phys. Rev. Lett. **72**, 3843 (1994).

[5] C. R. Natoli, M. Benfatto, C. Brouder, M. F. Ruiz Lopez, and D. L. Foulis, Phys. Rev. B **42**, 1944 (1990).

[6] S. Gota, R. Gunella, Z. Y. Wu, G. Jézéquel, C. R. Natoli, D. Sébilleau, E. L. Bullock, F. Proix, C. Guillot, and A. Quémerais, Phys. Rev. Lett. **71**, 3387 (1993).

[7] E. L. Bullock, R. Gunella, L. Patthey, T. Abukawa, S. Kono, C. R. Natoli, and L. S. Johansson, Phys. Rev. Lett. **74**, 2756 (1995).

[8] T. A. Tyson, K. O. Hodgson, C. R. Natoli, and M. Benfatto, Phys. Rev. B **46**, 5997 (1992).

[9] K. M. Schindler, V. Fritzsche, M. C. Asensio, M. C. Gardner, P. D. E. Ricken, A. W. Robinson, A. M. Bradschaw, D. P. Woodruff, J. C. Conesa, and A. Gonzalez-Elipe, Phys. Rev. B **46**, 4836 (1992).